INSTITUTE OF PHYSICS PUBLISHING PLASMA SOURCES SCIENCE AND TECHNOLOGY

Plasma Sources Sci. Technol. **10** (2001) 573–578 PII: S0963-0252(01)27383-6

Deposition of silicon dioxide films with a non-equilibrium atmospheric-pressure plasma jet

S E Babayan[1], J Y Jeong[1], A Schütze[1], V J Tu[1], Maryam Moravej[1], G S Selwyn[2] and R F Hicks[1,3]

[1] Chemical Engineering Department, University of California, Los Angeles, CA 90095, USA
[2] Plasma Physics Division, Los Alamos National Laboratory, Los Alamos, NM 87544, USA

E-mail: rhicks@ucla.edu

Received 9 May 2001, in final form 11 July 2001
Published 12 September 2001
Online at stacks.iop.org/PSST/10/573

Abstract

Silicon dioxide films were grown using an atmospheric-pressure plasma jet that was produced by flowing oxygen and helium between two coaxial metal electrodes that were driven by 13.56 MHz radio frequency power. The plasma exiting from between the electrodes was mixed with tetraethoxysilane (TEOS), and directed onto a silicon substrate held at 115–350 °C. Silicon dioxide films were deposited at rates ranging from 20 ± 2 to 300 ± 25 nm min^{-1}. The deposition rate increased with decreasing temperature and increasing TEOS pressure, oxygen pressure and RF power. For the latter two variables, the rate increased as follows: $Rd \propto P_{O_2}^{0.3}(RF)^{1.4}$. Films grown at 115 °C were porous and contained adsorbed hydroxyl groups, whereas films grown at 350 °C were smooth, dense and free of impurities. These results suggest that the mechanism in the atmospheric pressure plasma is the same as that in low-pressure plasmas.

1. Introduction

Silicon dioxide is one of the primary materials used in the fabrication of integrated circuits. These films are used as interlayer dielectrics and gate oxides in transistors [1–5], and are either grown by thermal oxidation of silicon [6], or deposited by thermal or plasma-enhanced chemical vapour deposition (PECVD) [7–11]. The latter method is preferred when deposition must be carried out at a low temperature. The PECVD of silicon dioxide is carried out using either silane, SiH_4, or tetraethoxysilane (TEOS), $Si(OC_2H_5)_4$. Although higher deposition rates are achieved with silane, better conformal coverage is obtained with TEOS due to its lower reactive sticking probability (0.045 compared to 0.35 for silane) [11]. In addition, TEOS is less hazardous and easier to handle. For these reasons, PECVD with TEOS is the preferred process for SiO_2 deposition in integrated circuit manufacturing [2, 5, 7, 12, 13].

We have recently developed an atmospheric-pressure plasma jet for use in materials processing [14–18]. The physics and chemistry of this device show similarities to that of low-pressure plasmas [19]. For example, the current–voltage curve of the plasma jet exhibits a Townsend dark region, followed by spark breakdown, a normal glow region, an abnormal glow region and, finally, arcing. This same behaviour has been observed in a low-pressure dc discharge [20]. In addition, normal glow occurs in both the jet and the dc discharge at currents from about 0.01 to 1.0 A and voltages between 100 and 400 V. Based upon a theoretical fit of the neutral Bremsstrahlung emission spectrum, it has been estimated that the density of charged particles in the atmospheric-pressure plasma jet ranges from 10^{11} to 10^{12} cm^{-3}, which is in the midrange of operation of low-pressure plasmas [19, 21]. On the other hand, the former discharge exhibits high concentrations of O atoms and ozone, both equal to approximately 10^{16} cm^{-3}. By contrast, the concentrations of these two species in low-pressure oxygen plasmas are about 10^{14} cm^{-3} and below 10^{10} cm^{-3}, respectively.

It is generally believed that oxygen atoms are active in the decomposition of TEOS during the CVD of silicon dioxide [11, 22–24]. Given that the O atom concentration in the plasma

[3] Author to whom correspondence should be addressed.

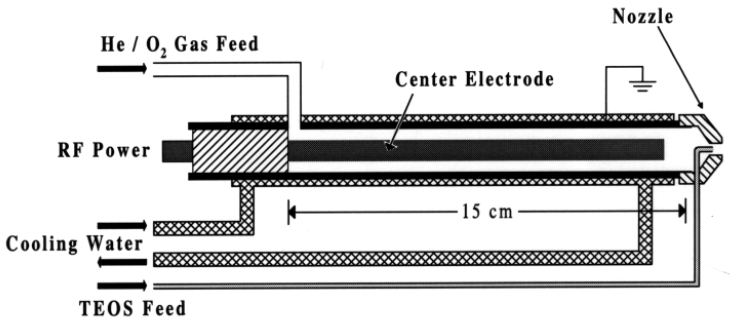

Figure 1. Schematic of the atmospheric-pressure plasma jet.

jet is so high, it was decided that this source may be well suited for the PECVD of SiO_2. Therefore, this process was studied thoroughly and an account of our findings is given below. In particular, the operating parameters used with the plasma jet affected the film growth rate and its properties in a way that is analogous to that observed in low-pressure plasmas. This reinforces the conclusion that O atoms are important reactive intermediates in the deposition of SiO_2 from TEOS.

2. Experimental methods

A schematic of the plasma jet is shown in figure 1 [15]. It consisted of two 14.5 cm long concentric electrodes made of stainless-steel. The inner diameter of the outer electrode was 1.6 cm, while the gap spacing was 0.16 cm. Oxygen and helium were passed through the annular space between the electrodes, and a plasma was generated by applying RF power at 13.56 MHz to the centre electrode. TEOS was added to the system by passing a small flow of helium through a bubbler that contained the volatile precursor. This mixture was injected into the plasma through a 0.16-cm tube fixed inside the nozzle at the end of the jet. The entire gas stream was directed onto a silicon wafer located 1.7 cm downstream.

The silicon dioxide films were deposited on p-type silicon substrates, 1.5 cm $\times$ 1.5 cm. These samples were cleaned by immersing them in boiling sulfuric acid for 5 min and dilute hydrofluoric acid for 30 s. After each acid dip, the samples were rinsed in deionized water. During deposition, the substrate holder was heated to between 115 and 350 °C, as measured by a thermocouple attached to the back of the sample. Unless otherwise noted, the standard process conditions were 757 Torr He, 3 Torr O_2, 7 mTorr TEOS, 115 °C, 280 W RF power and a total flow rate of 49 l min^{-1} (measured at 20 °C and 1 atm). Under these conditions, the transit time from the nozzle to the sample was 0.6 ms.

Film composition was examined by transmission infrared spectroscopy using a Bio-Rad FTS-40A spectrometer with a DTGS detector. An *ex situ* ellipsometer (Gaertner L116B) was used to measure the film thickness and the refractive index ($\lambda = 632$ nm); the psi and delta parameters were fitted by the software provided with the instrument (Gaertner LGEMP). The deposition rate was calculated by dividing the film thickness by the reaction time. The dielectric constants of several films were calculated from capacitance measurements, after constructing a parallel plate capacitor of known plate area and separation.

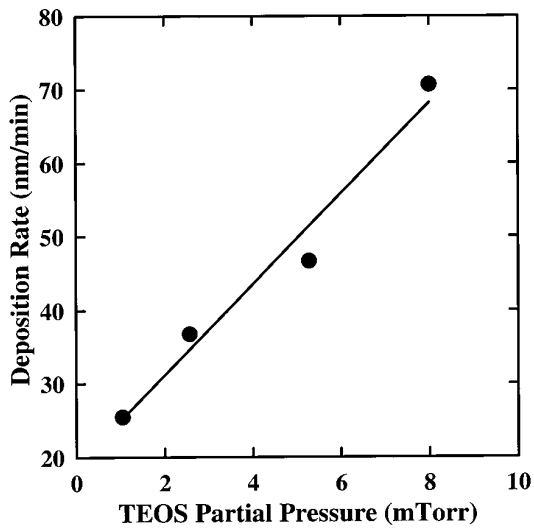

Figure 2. The dependence of the deposition rate on the TEOS partial pressure at 757 Torr He, 3 Torr O_2, 115 °C and 280 W RF power.

The film uniformity over the area used for the capacitance measurements was within 5 nm. Finally, several samples were imaged by atomic force microscopy (AFM), using an Autoprobe VP manufactured by Park Scientific Instruments.

3. Results

3.1. Deposition rate

The effect of the TEOS partial pressure on the deposition rate is shown in figure 2. The TEOS partial pressure is varied by changing the helium flow rate through the bubbler, while holding the bath temperature constant at 17 °C. The partial pressure is calculated assuming saturation of the vapour. Since the concentration of the TEOS in the jet effluent is not accurately measured by an independent technique, the trend in the figure should be taken as a qualitative indication of the effect of this process variable. Nevertheless, one sees that the deposition rate increases with the TEOS pressure throughout the range examined. Similar results have been reported for low-pressure PECVD processes [5, 23].

The effect of the oxygen partial pressure on the deposition rate is shown in figure 3. In this experiment the oxygen is fed between the electrodes and undergoes ionization. The

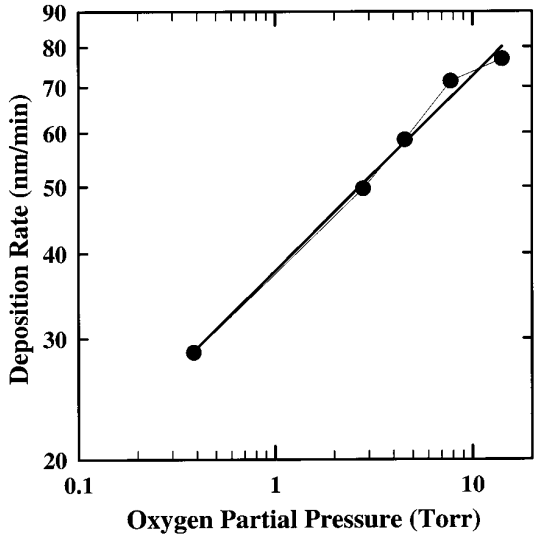

Figure 3. The dependence of the deposition rate on the oxygen partial pressure at 757 Torr He, 7 mTorr TEOS, 115 °C and 280 W RF power.

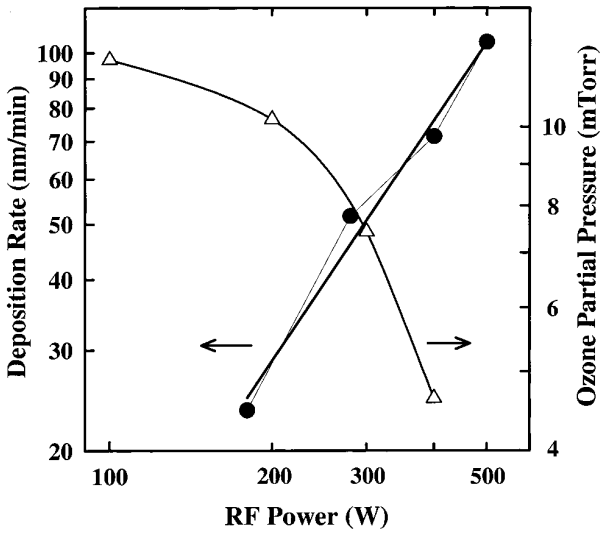

Figure 4. The dependence of the deposition rate and the ozone concentration on the RF power at 757 Torr He, 3 Torr O_2, 7 mTorr TEOS and 115 °C.

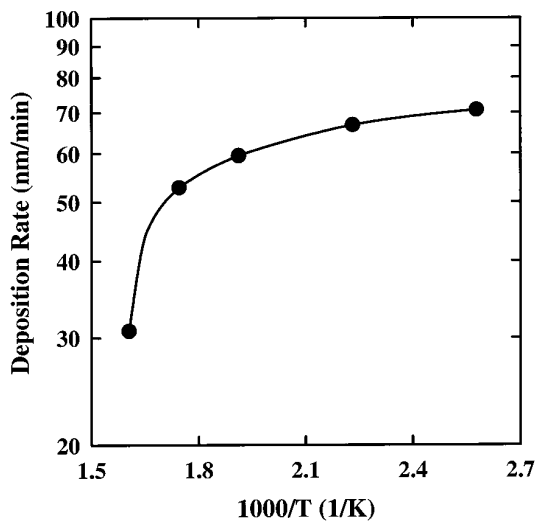

Figure 5. The dependence of the deposition rate on the substrate temperature at 757 Torr He, 3 Torr O_2, 7 mTorr TEOS and 280 W RF power.

deposition rate increases with the oxygen partial pressure, and, based on the slope of the log–log plot, the reaction order in O_2 is 0.3. The maximum amount of oxygen that can be fed through the plasma is 14 Torr. At higher pressures, the plasma extinguishes. In addition, it should be noted that if no oxygen is fed to the system the deposition rate falls to zero. Furthermore, adding 4 Torr O_2 through the nozzle, instead of upstream of the plasma, yields a deposition rate of only 10 nm min^{-1}.

Shown in figure 4 is the effect of the RF power on the deposition rate from 180 to 500 W. Below 180 W the deposition rate is too slow to be measured accurately, whereas above 500 W the jet arcs. The deposition rate exhibits a strong dependence on the RF power: the slope of the log–log plot equals 1.4. Also shown in figure 4 is the dependence of the ozone partial pressure on the RF power. The ozone pressure is measured at the exit of the nozzle using an electrochemical sensor [14]. One sees that this reaction product decreases rapidly with the applied power, in the opposite direction of the deposition rate. The maximum SiO_2 deposition rate obtained in this study is 300 ± 25 nm min^{-1} at 749 Torr He, 11 Torr O_2, 53 mTorr TEOS, 115 °C, 400 W and 41 l min^{-1} total flow. The TEOS pressure is calculated assuming saturation of the He gas passing through the bubbler at 200 cm^3 min^{-1} and a bath temperature of 30 °C.

A plot of the logarithm of the deposition rate as a function of the reciprocal temperature is shown in figure 5. The substrate temperature ranges from 115 to 350 °C. It is observed that the SiO_2 growth rate does not follow an Arrhenius relationship, but instead declines with increasing temperature. The drop in the rate is especially rapid between 275 and 350 °C. As discussed below, the substrate temperature also has a strong effect on the film properties.

3.2. Film properties

In figures 6(a) and 6(b), a series of transmission infrared spectra are presented of silicon dioxide films grown at different temperatures. In these figures, the specific absorbance was calculated by dividing the measured absorbance by the film thickness. The peaks at 450, 800 and 1080 cm^{-1} are due to the rocking, bending and asymmetric stretching modes of siloxane bridges, respectively [25–28]. The broad shoulder at $\sim$1200 cm^{-1} is also due to the asymmetric stretching vibrations of siloxane groups, although in this case, the Si–O–Si species are most likely located at a surface [26, 29]. At a surface, these groups are not subject to the dielectric screening effect, and so exhibit higher frequency stretching vibrations than their counterparts in the bulk [30]. The broad shoulder may also be due to OH incorporation in the form of silanol [27, 28, 31, 32].

Further examination of the infrared spectra reveals that some of them contain a well defined peak at 930 cm^{-1}, a broad band at 3400 cm^{-1} and a shoulder at 3650 cm^{-1}. These three features are due to hydroxyl groups. The peak at low frequency

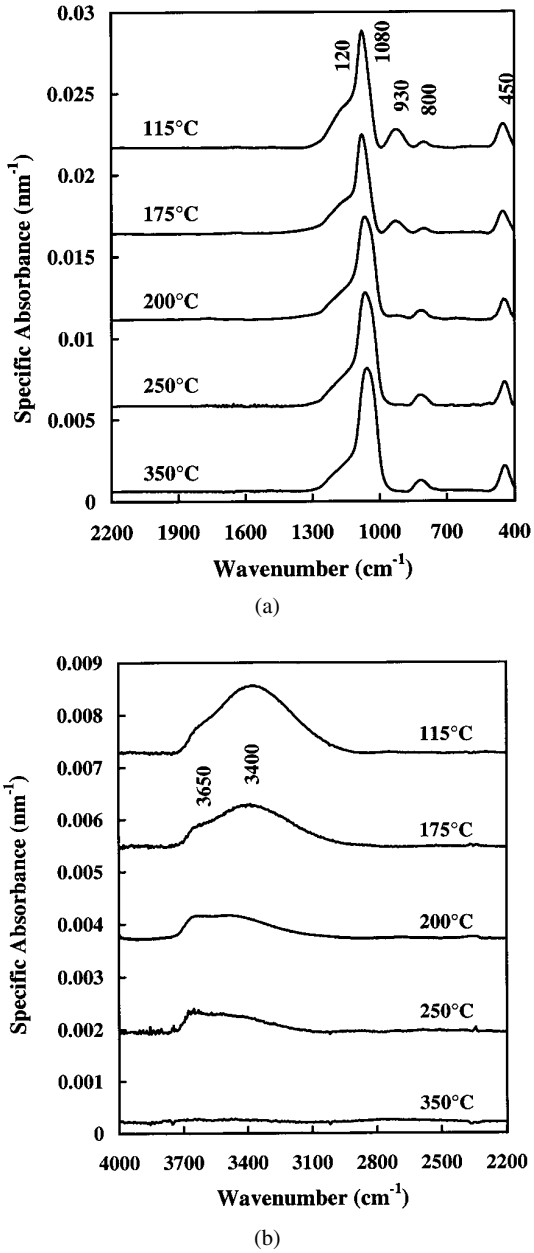

Figure 6. Transmission infrared spectra of SiO_2 films grown at temperatures between 115 and 350 °C: (a) 400–2200 cm^{-1} and (b) 2200–4000 cm^{-1}.

may be assigned to the O–H deformation mode, while the broad band and shoulder are due to the O–H stretching vibrations of hydrogen-bonded and isolated hydroxyl groups, respectively [32, 33]. It should be noted that no peaks are detected at 2900 and 1730 cm^{-1} due to C–H and C–O stretching vibrations, indicating that the ethoxide ligands do not incorporate into the film at any of the growth temperatures examined. Furthermore, the H_2O band at 1650 cm^{-1} is not observed.

It is evident from inspection of figures 6(a) and 6(b) that the compositions of the silicon dioxide films changes with deposition temperature. Increasing the temperature from 115 to 250 °C reduces hydroxyl incorporation and results in a significant decrease in the features at 930, 1200, 3400 and 3650 cm^{-1}, suggesting that the porosity of the films

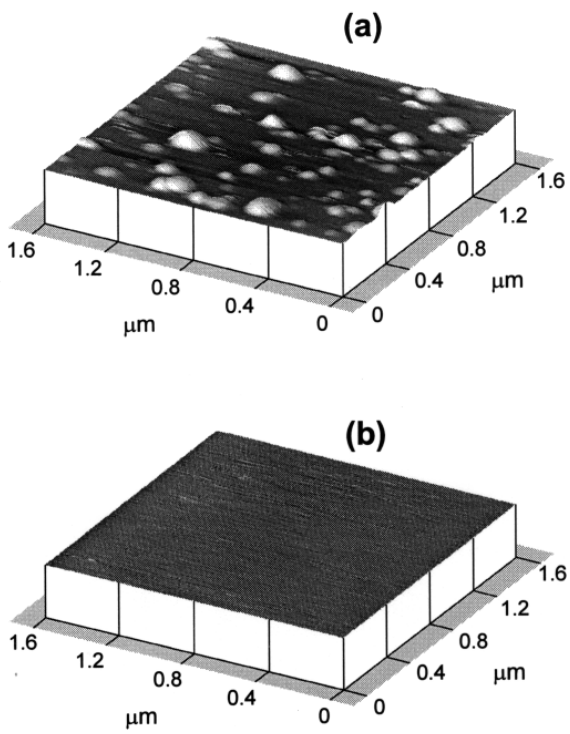

Figure 7. Atomic force micrographs of SiO_2 films grown at (a) 115 °C and (b) 350 °C. In (a) the z-axis is magnified by a factor of five to emphasize the surface topography.

has declined substantially. This decrease in porosity is a direct consequence of the reduction in hydroxyl incorporation [4, 26, 28, 29]. By 250 °C, these features are nearly absent from the spectrum. Evidently, $Si(OH)_x$ species are stable intermediates in the decomposition of TEOS by PECVD, and a relatively high substrate temperature is needed to drive the reaction all the way to SiO_2.

Atomic force micrographs of silicon dioxide layers deposited at 115 and 350 °C are presented in figure 7. The film grown at the lower temperature exhibits a peak-to-valley surface roughness of 230 nm, and one sees in the image white circular protrusions with diameters of 0.1–0.3 μm. These protrusions most likely cover over large voids within the film. This is consistent with the infrared results, which indicate that the material is porous. Moreover, several researchers have reported that voids are present in silicon dioxide films grown by PECVD below 200 °C [1, 34]. In contrast to the results obtained at low temperature, the film deposited at 350 °C has a much smoother surface. No features are discernable in the AFM image, figure 7(b), and the peak-to-valley surface roughness is only 20 Å.

The refractive index of the silicon dioxide films, as measured by ellipsometry, does not show a significant dependence on the process parameters. For most samples, the refractive index equals 1.45 ± 0.02. Based on capacitance measurements, the dielectric constant of the films ranged from 5.0 ± 0.2 for deposition below 150 °C to 3.81 ± 0.03 for deposition at 350 °C. The uncertainty in these values represents the standard deviation for at least four repeat

measurements. The higher dielectric constant observed for growth at lower temperatures is consistent with the incorporation of hydroxyl groups in the film [35]. The dielectric constant of silica has been found to obey the equation: $\varepsilon = 3.8073 + 2.72 \times 10^{-22} \times N$, where N is the concentration of hydroxyl groups per cm^{-3} [35]. From this relationship, the hydroxyl concentration is calculated to be 4.38×10^{21} cm^{-3} for the film deposited at 150 °C. In contrast, the SiO_2 film grown at 350 °C is, to within the error of the measurement, free of hydroxyl impurities.

4. Discussion

The PECVD of silicon dioxide has been well studied in low-pressure plasmas [4, 5, 23, 36–38]. It has been found that the deposition rate increases with oxygen partial pressure and RF power, but decreases with increasing temperature. These results have been explained by a two-step reaction mechanism. First TEOS and O atoms react to produce silicon hydroxide:

$$Si(OC_2H_5)_4 + 4O \Leftrightarrow Si(OH)_4 + 4C_2H_4O.$$

This reaction represents a sequence of four elementary steps, each involving the collision of an O atom with $Si(OH)_n(OC_2H_5)_{4-n}$ molecules, where $n = 0$, 1, 2 or 3. The second step in the mechanism is the adsorption of TEOS, or one of the $Si(OH)_n(OC_2H_5)_{4-n}$ intermediates. The oxidation of the ethoxide ligand can occur either before or after adsorption of the precursor.

Due to the low sticking probability of the precursor, adsorption is the rate-limiting step in the deposition process [11]. A low sticking probability is essential to achieve conformal coverage of SiO_2 in trenches and other integrated circuit features. Since the molecules collide with the walls of the trenches many times before a reaction occurs, they can attain a uniform concentration throughout the trench, and hence provide a uniform deposition rate [5]. Furthermore, it is known from precursor-state adsorption kinetics that the reactive sticking probability of a molecule declines with increasing temperature, consistent with the trend observed in figure 5 [39].

The deposition of silicon dioxide with the atmospheric-pressure plasma jet most likely follows the same reaction mechanism as described above for low-pressure PECVD. The growth rate obtained with the plasma jet shows a positive dependence on O_2 pressure and RF power, and a negative dependence on temperature (cf figures 3, 4 and 5). In other work, we have shown that the O atom concentration is high, $\sim 10^{16}$ cm^{-3}, and increases with the O_2 partial pressure [19, 40]. The plasma jet also produces significant amounts of ozone, $\sim 10^{16}$ cm^{-3}, and metastable molecular oxygen, $\sim 10^{15}$ cm^{-3}, a $^1\Delta_g$ state. Nevertheless, the ozone concentration is too low to produce an appreciable rate of reaction with the TEOS. The maximum ozone concentration recorded in the jet effluent was 300 ppm, whereas SiO_2 CVD with TEOS and ozone is carried at concentrations of 1.0 vol% O_3 [3, 41]. In addition, in figure 4 one sees that the deposition rate and the ozone partial pressure follow opposite trends with the RF power. With regard to metastable molecular oxygen, we cannot entirely rule out its participation in the reaction. However, it is a much 'weaker' oxidant than O atoms, and is at a lower initial concentration.

In low-pressure plasma reactors, silicon dioxide films are deposited at a minimum temperature of 375 °C [4, 23, 37]. At lower temperatures, the SiO_2 layers incorporate significant quantities of hydroxyl groups and tend to be porous. Patrick *et al* [4] reported that silicon dioxide films deposited at 390 °C in a commercial low-pressure PECVD reactor exhibited a dielectric constant of 4.10 ± 0.05. Hydroxide contamination is also a problem with SiO_2 films produced with the atmospheric-pressure plasma jet. However, in this case, growth at 350 °C is sufficient to reduce the OH content to below the detection limit of the infrared spectrometer (cf figure 6). In addition, the dielectric constant of the SiO_2 films deposited at 350 °C is 3.81 ± 0.03. These results suggest that the atmospheric-pressure plasma jet may produce films of superior quality to those obtained in low-pressure plasma reactors.

Another problem observed in low-pressure plasmas is the incorporation of organic species in the films. This results from electron collisions with the ethoxide ligands, causing them to dissociate into CH_x fragments [11]. The organic impurities are reduced to a minimum by operating at an oxygen to TEOS mole ratio above 5.0 [4]. In the present work, infrared bands due to C–H stretching vibrations are not detected in any of the glass films. Eliminating the oxygen feed from the plasma simply reduces the growth rate to zero. Evidently, electron–TEOS collisions are not significant in the effluent of the plasma jet. We have taken Langmuir probe measurements 5 mm downstream of the nozzle, and they indicate a charged particle flux of 10^{14} cm^{-2} at 100 W power [14]. This is already several orders of magnitude lower than the precursor flux required to yield the observed growth rate under these conditions.

It has been reported that the addition of small amounts of hydrogen to low-pressure plasmas can reduce the incorporation of hydroxyl groups and organic impurities in the SiO_2 films [42]. Several experiments were conducted in which about 2 Torr of H_2 was added either upstream through the plasma, or downstream to the nozzle. The addition of hydrogen to the nozzle had no effect on the deposition process. However, the addition of hydrogen to the plasma completely inhibited silicon dioxide film growth. Further experiments are needed to determine what effect hydrogen has on the reactive oxygen species generated within the plasma.

5. Conclusions

Silicon dioxide has been deposited by mixing TEOS with the effluent of an oxygen plasma jet operated at atmospheric pressure. The mechanism of SiO_2 deposition with the plasma jet appears to be the same as that observed in low-pressure PECVD processes. In particular, the TEOS decomposes by a two-step process, involving a reaction with O atoms to produce silanol intermediates, followed by the decomposition of these intermediates on the film surface into SiO_2. Below 400 °C, the films generated with the atmospheric-pressure plasma jet contain fewer impurities than those generated in low-pressure PECVD reactors. In the latter case, electron-impact dissociation of the ethoxide ligands promotes the incorporation of impurities. In contrast, the plasma jet effluent contains an extremely low concentration of electrons and ions.

Acknowledgments

This work was supported by the National Science Foundation, Division of Chemical and Transport Systems, and the US Department of Energy, Environmental Management Sciences Program.

References

[1] Ceiler M F Jr, Kohl P A and Bidstrup S A 1995 *J. Electrochem. Soc.* **142** 2067
[2] Ikeda K, Nakayama S and Maeda M 1996 *J. Electrochem. Soc.* **143** 1715
[3] Murase K 1994 *Japan. J. Appl. Phys.* **33** 1385
[4] Patrick W J, Schwartz G C, Chapple-Sokol J D, Carruthers R and Olsen K 1992 *J. Electrochem. Soc.* **139** 2604
[5] Ray S K, Maiti C K, Lahiri S K and Chakrabarti N B 1996 *Adv. Mater. Opt. Electron.* **6** 73
[6] Balk P 1988 *The Si–SiO_2 System* (Amsterdam: Elsevier)
[7] Raupp G B, Shemansky F A and Cale T S 1992 *J. Vac. Sci. Technol.* B **10** 2422
[8] Yasuda N, Takagi S-i and Toriumi A 1997 *Appl. Surf. Sci.* **117/118** 216
[9] Adams A C, Reif R and Srinivasan G R 1986 *Reduced Temperature Processing for VLSI* (Pennington, NJ: Electrochemical Society)
[10] Becker F S, Pawlik D, Anzinger H and Spitzer A 1987 *J. Vac. Sci. Technol.* B **5** 1555
[11] Lieberman M A and Lichtenberg A J 1994 *Principles of Plasma Discharges and Materials Processing* (New York: Wiley)
[12] Ong T P, Tobin P and Mele T 1995 *J. Appl. Phys.* **77** 6055
[13] Helms C R and Poindexter E H 1994 *Rep. Prog. Phys.* **57** 791
[14] Jeong J Y, Babayan S E, Tu V J, Park J, Henins I, Hicks R F and Selwyn G S 1998 *Plasma Sources Sci. Technol.* **7** 282
[15] Babayan S E, Jeong J Y, Tu V J, Park J, Selwyn G S and Hicks R F 1998 *Plasma Sources Sci. Technol.* **7** 286
[16] Jeong J Y, Park J Y, Henins I, Babayan S E, Tu V J, Selwyn G S, Ding G S and Hicks R F 2000 *J. Phys. Chem.* A **104** 8027
[17] Tu V J, Jeong J Y, Schütze A, Babayan S E, Selwyn G S, Ding G S and Hicks R F 2000 *J. Vac. Sci. Technol.* A **18** 2799
[18] Jeong J Y, Babayan S E, Schütze A, Tu V J, Park J Y, Henins I, Selwyn G S and Hicks R F 1999 *J. Vac. Sci. Technol.* A **17** 2581
[19] Schütze A, Jeong J Y, Babayan S E, Park J, Selwyn G S and Hicks R F 1998 *IEEE Trans. Plasma Sci.* **26** 1685
[20] Francis G 1956 The glow discharge at low pressure *Encyclopedia of Physics: Gas Discharges II* vol XXII, ed S Flügge, pp 53–208
[21] Park J, Hennins I, Herrmann H W and Selwyn G S 2000 *J. Appl. Phys.* **7** 3141
[22] Kawahara T, Yuuki A and Matsui Y 1992 *Japan. J. Appl. Phys.* **31** 2925
[23] Mukherjee S P and Evans P E 1972 *Thin Solid Films* **14** 105
[24] Wickramanayaka S, Matsumoto A, Nakanishi Y, Hosokawa N and Hatanaka Y 1994 *Japan. J. Appl. Phys.* **33** 3520
[25] Colthrup N B, Daly L H and Wiberley S E 1964 *Introduction to Infrared and Raman Spectroscopy* (New York: Academic)
[26] Chou J-S and Lee S-C 1995 *J. Appl. Phys.* **77** 1805
[27] Haque M S, Naseem H A and Brown W D 1997 *J. Electrochem. Soc.* **144** 3265
[28] Montero I, Galán L, Najmi O and Albella J M 1994 *Phys. Rev.* B **50** 4881
[29] Fogarassy E, Slaoue A, Fuchs C and Regolini J L 1987 *Appl. Phys. Lett.* **51** 337
[30] Wagner H and Beyer W 1983 *Solid State Commun.* **48** 585
[31] Goullet A, Vallée C, Granier A and Turban G 2000 *J. Vac. Sci. Technol.* A **18** 2452
[32] Theil J A, Tsu D V, Watkins M W, Kim S S and Lucovsky G 1990 *J. Vac. Sci. Technol.* A **8** 1374
[33] Bellamy L J 1958 *The Infra-Red Spectra of Complex Molecules* (New York: Wiley)
[34] Adams A C, Alexander F B, Capio C D and Smith T E 1981 *J. Electrochem. Soc.* **128** 1545
[35] Andeen C, Schuele D and Fontanella J 1974 *J. Appl. Phys.* **45** 1071
[36] Sano K, Hayashi S, Wickramanayaka S and Hatanaka Y 1996 *Thin Solid Films* **281–282** 397
[37] Pai C S and Chang C-P 1990 *J. Appl. Phys.* **68** 793
[38] Webb D A, Lane A P and Tang T E 1989 *Proc. 2nd Int. Symp. on Ultra Large Scale Integration Science and Technology, 175th, Meeting of the Electrochemical Society (May 1989)* (Pennington, NJ: Electrochemical Society)
[39] Weinberg W H 1991 *Dynamics of Gas–Surface Collisions* ed M N R Ashfold and C T Rettner (Cambridge: Royal Society of Chemistry)
[40] Jeong J Y, Babayan S E, Tu V J, Schütze A, Park J, Henins I, Hicks R F and Selwyn G S, unpublished results
[41] Nguyen S, Dobuzinsky D, Harmon D, Gleason R and Fridmann S 1990 *J. Electrochem. Soc.* **137** 2209
[42] Ha H, Inomata K and Koinuma H 1995 *J. Electrochem. Soc.* **142** 2726